Biochemical Pharmacology 225 (2024) 116264

Contents lists available at ScienceDirect

Biochemical Pharmacology

journal homepage: www.elsevier.com/locate/biochempharm

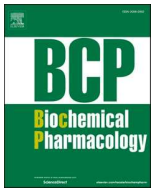

Modulation of contextual fear acquisition and extinction by acute and chronic relaxin-3 receptor (RXFP3) activation in the rat retrosplenial cortex

Mónica Navarro-Sánchez [a,1], Isis Gil-Miravet [a,1], Daniel Montero-Caballero [a], Ross A.D. Bathgate [b,c,d], Mohammed Akhter Hossain [b,c], Esther Castillo-Gómez [a,e], Andrew L. Gundlach [b,c], Francisco E. Olucha-Bordonau [a,e,*]

[a] Departamento de Medicina, Facultad de Ciencias de La Salud, Universitat Jaume I, Castellón, Spain
[b] The Florey Institute of Neuroscience and Mental Health, The University of Melbourne, Victoria, Australia
[c] Florey Department of Neuroscience and Mental Health, The University of Melbourne, Victoria, Australia
[d] Department of Biochemistry and Pharmacology, The University of Melbourne, Victoria, Australia
[e] CIBERsam-isciii, Red Española de Estrés, Spain

ARTICLE INFO

Keywords:
Neuropeptide modulation
G-protein-coupled receptor (GPCR)
Emotion
GABA
Glutamate
Excitatory/inhibitory balance

ABSTRACT

The retrosplenial cortex (RSC) plays a central role in processing contextual fear conditioning. In addition to corticocortical and thalamocortical projections, the RSC receives subcortical inputs, including a substantial projection from the nucleus incertus in the pontine tegmentum. This GABAergic projection contains the neuropeptide, relaxin-3 (RLN3), which inhibits target neurons via its Gi/o-protein-coupled receptor, RXFP3. To assess this peptidergic system role in contextual fear conditioning, we bilaterally injected the RSC of adult rats with an adeno-associated-virus (AAV), expressing the chimeric RXFP3 agonist R3/I5 or a control AAV, and subjected them to contextual fear conditioning. The R3/I5 injected rats did not display any major differences to control-injected and naïve rats but displayed a significantly delayed extinction. Subsequently, we employed acute bilateral injections of the specific RXFP3 agonist peptide, RXFP3-Analogue 2 (A2), into RSC. While the administration of A2 before each extinction trial had no impact on the extinction process, treatment with A2 before each acquisition trial resulted in delayed extinction. In related anatomical studies, we detected an enrichment of RLN3-immunoreactive nerve fibers in deep layers of the RSC, and a higher level of co-localization of RXFP3 mRNA with vesicular GABA transporter (vGAT) mRNA than with vesicular glutamate transporter-1 (vGLUT1) mRNA across the RSC, consistent with an effect of RLN3/RXFP3 signalling on the intrinsic, inhibitory circuits within the RSC. These findings suggest that contextual conditioning processes in the RSC involve, in part, RLN3 afferent modulation of local inhibitory neurons that provides a stronger memory acquisition which, in turn, retards the extinction process.

1. Introduction

Relevant information from the external and internal environment is codified, stored, and retrieved through brain learning and memory processes. The retrosplenial cortex (RSC) is one of the key regions participating in the associated complex neural circuits. Pathological alterations in tau protein(s) within the RSC are associated with the first clinical signs of Alzheimer's disease [1] and these alterations occur

Abbreviations: A2, RXFP3-Analogue 2; A2-AC, A2 infusion prior to each acquisition session; A2-EXT, infusion of A2 prior to each extinction session; AAV, Adeno-associated-virus; aCSF, Artificial cerebrospinal fluid; CHO, Chinese hamster ovary; CREB, cAMP-responsive element binding protein; Fmoc, N-(9 fluorenyl) methoxycarbonyl; GPCR, G-protein-coupled receptor; ISH RNAscope™, Multiplex *in situ* hybridization; NI, Nucleus incertus; PKA, protein kinase A (PKA); PostS1, Post-shock time of the first acquisition session; PostS2, Post-shock time of the second acquisition session; PreS1, Pre-shock time of the first acquisition; PreS2, Pre-shock time of the second acquisition session; PTSD, Post-traumatic stress disorder; R3/I5 group, AAV1/2-sCAG:R3/I5-IRES-eGFP; RLN3, Relaxin 3; RSC, Retrosplenial cortex; RXFP3, Relaxin-3 receptor; T1, First extinction test; T2, Second extinction test; T3, Third extinction test; T4, Fourth extinction test; US, Unconditioned stimulus; vGAT, Vesicular GABA transporter; vGLUT1, Vesicular glutamate transporter-1.

* Corresponding author at: UP Medicina, Facultad de Ciencias de la Salud, Universitat Jaume I, Av Vicent Sos Baynat sn, 12071 Castellón, Spain.
E-mail address: folucha@med.uji.es (F.E. Olucha-Bordonau).

[1] Equal contribution

https://doi.org/10.1016/j.bcp.2024.116264
Received 16 January 2024; Received in revised form 30 April 2024; Accepted 3 May 2024
Available online 4 May 2024

before the clinical signs of disease [2]. Moreover, hemorrhagic lesions circumscribed to the RSC result in anterograde and retrograde amnesia [3]. In fact, lesion studies indicate that the RSC is necessary for spatial learning and navigation, and that these functions require the integrity of the circuit interconnecting the RSC with the anterior thalamic nuclei and the hippocampus, as combined pairs of lesions are much more effective to impair these spatial learning and navigation [4].

In rodents, the RSC occupies a large cortical extension and is centrally positioned between cortical sensory areas and the hippocampal formation integrating egocentric and allocentric spatial information to configure contextual perception [5]. Contextual fear conditioning is a complex form of Pavlovian conditioning in which a set of external and internal stimuli are presented together as an engram and become associated with an unpleasant, unconditioned stimulus. The perception of the context as a set, then, acquires emotional predictive value [6,7], and the RSC is a key node for processing contextual fear conditioning [8].

Data from studies involving inactivation of the RSC indicate a central role for neural processing in the RSC in the recall of contextual memories. Indeed, lesions either pretraining or post training led to a reduction in the conditioned responses after re-exposure to the same context [9]. In fact, specific inactivation of glutamatergic neurons in the deep layers of the RSC impaired the recall of contextual memories [10]. Moreover, optogenetic re-activation of contextual-specific neural engrams in the RSC tagged using c-Fos promotors, is able to produce conditioned responses [11]. Furthermore, it has been reported that the RSC is highly involved in the retrieval of remote contextual memories [7]. Notably, while there are only minor effects of the RSC on cued fear conditioning when the test is done close to the acquisition trials, there is an impairment of conditioned responses when retrieval is tested ≥ 1 month after acquisition [12]. Thus, remote retrieval of cued conditioning appears to be RSC-dependent. In contrast, acquisition and retrieval of trace-fear conditioning can be impaired by manipulations of the RSC, including blocking protein synthesis during acquisition or blocking NMDA receptors during retrieval [13].

In addition to the specific association between the context (as a set of the environmental and internal elements that meet in a particular moment) and the unconditioned stimulus (US), the context may configure an association with a cue as a unique configuration [14] and the RSC plays a role in these associations. For example, pre-exposure to a cue (i.e., latent inhibition, which is context-dependent) prevents the association between the cue and the US and elicits neural activity in the RSC. Under these conditions, after context extinction, there is an enhancement of conditioned responses to the cue and, at the same time, there is an enhancement of RSC activity to the pre-exposed cue. These results suggest a central role for the RSC in the contextual coding of latent inhibition [15].

During contextual fear conditioning, there is a change in the coherence pattern of the oscillatory neural activity at theta frequency between the RSC *and* the hippocampus, the anterior cingulate cortex and the anterodorsal thalamus, with an increased coherence during encoding, retrieval and extinction [16]. Moreover, coherence between the RSC and the hippocampus is decreased during retrieval of remote contextual memories, which was interpreted as a loss of dependency on the hippocampal-RSC interaction under those conditions [15,17].

Of interest to our research, a prominent ascending projection that targets the RSC *and* septohippocampal system arises from the *nucleus incertus* (NI) in the pontine tegmentum [17,18]. Furthermore, the abundant GABAergic NI projections are well recognized as delivering the neuropeptide, relaxin-3 (RLN3) to distant nerve terminal [19]. The distribution pattern of RLN3-positive nerve fibers [20,21] correlated quite well with the distribution of efferents from the NI assessed using neural tract tracers [17,18,22]. Both, electric stimulation of the NI and direct infusion of an RLN3 agonist peptide into the medial septum induces hippocampal theta [23–25]. Lesion of the NI induces a retardation of the extinction of a cue that previously paired with a shock [26] and extinction is a context dependent procedure. In addition, it has been demonstrated that activation of NI GABAergic neurons is able to impair contextual fear memory acquisition and this impairment is mediated through somatostatin interneurons of the CA1. Thus, it was concluded that NI action was filtering non-salient contextual information and enhancing relevant incoming contextual features [27].

RLN3 belongs to the relaxin-family of peptides and is present in all vertebrate taxa [28]. Soon after its discovery, RLN3 was identified as the cognate ligand for the brain-enriched, $G_{i/o}$-protein-coupled receptor, GPCR135 [29], which was subsequently renamed relaxin-family peptide-3 receptor (RXFP3) [30]. Activation of RXFP3 inhibits adenylate cyclase-induced cellular accumulation of cAMP [29], and induces the phosphorylation of ERK *in vitro* [31] and *in vivo* [32]. In recent functional studies, the genetic deletion of RXFP3 in hippocampus [33] or medial septum [34] in adult $Rxfp3^{loxP/loxP}$ mice, impaired spatial memory. However, the effects of alterations in RXFP3 activity in RSC on learning and memory have not been explored.

In this study, we hypothesized that the strong NI RLN3 projection to the RSC plays a role in processing the perception of context and participates in its Pavlovian association to an unconditioned stimulus. In studies to explore this hypothesis, we used an AAV that produces the R3/I5 agonist peptide, specific for RXFP3, which is locally secreted by RSC neurons. The AAV1/2-sCAG:R3/I5-IRES-eGFP vector has been employed in previous studies that revealed an RXFP3-related, sustained regulation of food intake, body weight and reduced peptide hormone expression in the hypothalamus of adult rats [35] and increased levels of anxiety-like behavior following chronic expression and secretion of R3/I5 in the ventral hippocampus of adult, male rats [36]. In addition, we injected the selective RXFP3 agonist peptide, RXFP3-Analogue 2 (A2) [37] into the RSC, just before acquisition or during retrieval and extinction, to determine whether enhanced RXFP3 signalling participated in acquisition, retrieval or extinction mechanisms. Finally, we mapped the location of RLN3-positive nerve fibers and RXFP3 mRNA-positive neurons in the different layers of area 29 and area 30 of the RSC, and the relative localisation of RXFP3 transcripts in GABAergic and glutamatergic neurons by detecting the co-localisation of RXFP3 mRNA with vesicular GABA transporter (vGAT) or vesicular glutamate transporter-1 (vGLUT1) mRNA.

2. Experimental procedures

2.1. Animals

This study used a total of 38 male Wistar rats (Janvier, Le Genest-Saint-Isle,France) weighing 300–510 g. Rats were housed in groups of 2–3 rats per cage for a 7 days period. After surgery, rats were single-housed with food and water available ad libitum. Rats were individually housed and held in a temperature and humidity controlled colony room on a regular 12 h light–dark cycle with lights on at 8 am. All experiments were conducted during the light phase.

All experimental procedures were approved by the Animal Welfare Ethics Committee of the Universitat Jaume I, Castellón (Spain) and developed in accordance with the European Community Council Directive (86/609/EEC; 2010/63/EU), Spanish directive BOE 34/11370/2013, and local directive DOGV 26/2010.

2.2. Surgery

Rats were anaesthetised with isoflurane (Isoflutek, 1000 mg/g, Karizoo, Barcelona, Spain) (1.5–2 % in oxygen) and placed in a stereotaxic apparatus (David Kopf Instruments, Tujunga, CA, USA). The skin covering the skull was separated, and holes were drilled in the skull targeting the RSC at stereotaxic coordinates relative to bregma: AP –6.5 mm, ML ± 0.8 mm, DV –2.2 mm. For recovery after surgery, all rats were administered Meloxicam (Metacam® Boehringer-Ingelheim Vetmedica GmbH, Rhein Germany) at a dosage of 0.5 mg in 0.1 ml for two days.

2.2.1. AAV injections

Using a 1 μL Hamilton syringe, we infused 0.75 μl (0.2 μl/min) of AAV1/2-sCAG:R3/I5-IRES-eGFP particles (8 x 10^{11} gc/ml) (n = 7) or AAV1/2-sCAG-IRES-eGFP particles (2 x 10^{11} gc/ml) (n = 6) into the RSC of rats at a rate of 0.5 μL/min and both particles were allowed to diffuse for 10 min before the syringe was slowly removed. Subsequently, the incision was sutured, and the rat was returned to its cage for recovery (see Fig. 1).

2.2.2. Guide cannula placement

For indwelling guide cannula implantation (n = 24), a stainless-steel guide cannula (21-gauge) was positioned and implanted in the RSC using surgical screws and dental cement. Subsequently, rats were housed in individual cages (see Fig. 2).

2.3. Peptide synthesis

The RXFP3 agonist peptide A2 was synthesized as described [37]. In brief, the A- and B-chains are prepared by continuous flow Fmoc (N-(9 fluorenyl)methoxycarbonyl)-solid phase peptide synthesis [38,39]. Directed disulfide bond formation was achieved by the selection and use of appropriate S-protection groups [40,41] which were subsequently removed in a stepwise fashion to individually form each of the two disulfide bonds. The two-chain peptide A2 was purified using RP-HPLC and its identity and purity were confirmed by RP-HPLC and MALDI-TOF MS.

2.4. Apparatus

The conditioning apparatus used consisted of two fear chambers (28 × 21 × 26 cm; Model 80015, Lafayette Instruments, Lafayette, IN, USA) with a camera installed in the top to record behavior. The chambers were equipped with a stainless-steel shock-delivery grid floor (0.9 cm inter-bar separation) and two dim lights. The equipment was calibrated to deliver discharges with an amplitude of 0.3 mA and a duration of 0.5 s (Lafayette Instruments). The timing of shock administration was established prior to the start of the behavioral sessions and was automatically administered through a shocker fitted with an Arduino card (Uno R3, Ivrea, Italy) using customized software (HackCS, Castellón, Spain). The apparatus was cleaned with 30 % ethanol before and after each rat was tested.

2.5. Contextual fear conditioning protocol

All rats had two handling sessions during the two days prior to the behavioral experiment. The process was divided into sessions of 10 min (2 acquisition and 4 extinction sessions) across three days. One extra extinction session was added for the RXFP3 agonist experiment.

Day 1 – Acquisition. In the first session, 2 h after the start of the light cycle, rats received an electric shock after 4 min in the conditioning box. In the second session, at least four hours later, the shock was applied after 6 min in the conditioning boxes.

Day 2 and 3 – Extinction. On day 2, the rats were returned to the conditioning box for extinction sessions 1 and 2, and the sessions were spaced 4 h apart. During these sessions, the rats were placed in the boxes with the same context, but without shock for a total of 10 min. On day 3, the same procedure as day 2 was repeated for extinction sessions 3 and 4. For the RXFP3 agonist experiment, on day 4 rats were returned to the conditioning box for extinction session 5.

2.5.1. Effect of chronic RXFP3 agonist secretion in RSC on contextual fear conditioning

Previous studies have shown that three weeks after the AAV injection is sufficient to produce a behavioral effect, and we delayed studies for a further week to ensure optimal AAV expression [35,36]. In our experiments, rats performed the contextual fear conditioning behavioral protocol 1 month after injection of AAV1/2-sCAG:R3/I5-IRES-eGFP (R3/I5 group) or AAV-sCAG-IRES-eGFP (SHAM group) (see Fig. 1).

2.5.2. Effect of acute RXFP3 agonist administration into RSC on acquisition and extinction of contextual fear conditioning

Three groups of rats performed the behavioral protocol 4 days after guide cannula implantation. Group 1 received an A2 infusion 15 min prior to each acquisition session and an infusion of aCSF prior to each extinction session (A2-AC); group 2 received an aCSF infusion 15 min prior to acquisition and an infusion of A2 15 min prior to each extinction session (A2-EXT); and group 3 received an aCSF infusion 15 min prior to all sessions (SHAM). A solution of 40 pmol/μl A2 was used and 0.5 μl of A2 or aCSF was administered at a rate of 0.25 μl/min.

2.6. Multiplex RNAscope™ in situ hybridization

Multiplex *in situ* hybridization (ISH; RNAscope™) was performed as described by Advanced Cell Diagnostics (ACD, Newark, CA, USA) (see also [42,45]). Four naïve rats were deeply anesthetized with sodium pentobarbital (Dolethal, 200 mg/kg, i.p., Vetoquinol S.A., Madrid, Spain), and decapitated. Brains were rapidly removed and rapidly frozen over liquid nitrogen isopentane (Sigma-Aldrich, St Louis, MO, USA) and stored at –80 °C until further processing. Brains were warmed to –20 °C for 2 h and then mounted in a cryostat (Cryocut CM 1800, Leica Microsystems, Wetzlar, Germany). Coronal sections (16 μm) were cut and thaw-mounted on Superfrost-Plus Slides (Fisher Scientific, Hampton, NH, USA, Cat#12-550-15).

Slides were transferred to cold (4 °C) 4 % paraformaldehyde for 15 min then rinsed in 0.01 M PBS, and dehydrated in increasing ethanol concentrations (50, 70 and 100 %). Once dehydrated the sections were stored in 100 % ethanol overnight at –20 °C. Slides were then air-dried, and a hydrophobic barrier was drawn around the sections (ImmEdge hydrophobic PAP pen, Vector Laboratories, Burlingame, CA, USA; Cat #310018). Sections were incubated with protease pre-treatment 4 (ACD, Cat #322340) for 16 min. After a PBS rinse, sections were incubated for 2 h at 40 °C with three different probe combinations targeting (i) RXFP3 (ACD, #316181), (ii) vGLUT1 (Slc17a6; ACD, #317011) and (iii) vGAT (Slc32a1; ACD, #424541) mRNA. Following incubation, sections were rinsed with wash buffer (ACD, Cat#310091) and signals were amplified with ACD amplifier reagents according to the manufacturer's protocol. After 2 rinses in wash buffer, sections were stained with DAPI (ACD, #320851) and coverslipped using Mowiol (Sigma-Aldrich).

2.7. Image acquisition and analysis

Immunofluorescent multiplex ISH images were captured with a confocal microscope (Leica DMi8, Leica Microsystems CMS GmbH, Wetzlar, Germany). Analysis images were captured with 40 × lenses and resolution of 512 × 512 dpi. Quadruple-labelling was captured with lasers 405 (laser intensity: 3.0 %; gain: 775; offset: –2) 488 (laser intensity: 6.0 %; gain: 750; offset: –2), 561 (laser intensity: 0.3 %; gain: 50; offset: 0), 633 (laser intensity: 3.0 %; gain: 750; offset: –2) that were constant for each analysis. Each image was formed by a stack of 10 images of 1.5 μm and the tilescan option for all RSC regions, and then a mosaic merge and maximal projection process was applied using the Leica Application Suite LAS X (Leica Microsystems). Individual images for illustrative purposes were captured with 63 × objective and stacks of 1.5 μm through the entire cell.

Quantification of the relative neuronal co-localization of RXFP3, vGLUT1, and vGAT mRNA (with DAPI) was conducted automatically using QuPath 0.4.3 (https://qupath.github.io/). Images were subdivided for RSC areas (29a, 29b, 29c, and 30) and cortical layers (I, II/III, IV, V, and VI) using different ROIs and then counted automatically using the 'Create single measurement classifier' feature within the object classification in QuPath. This tool is designed for the precise

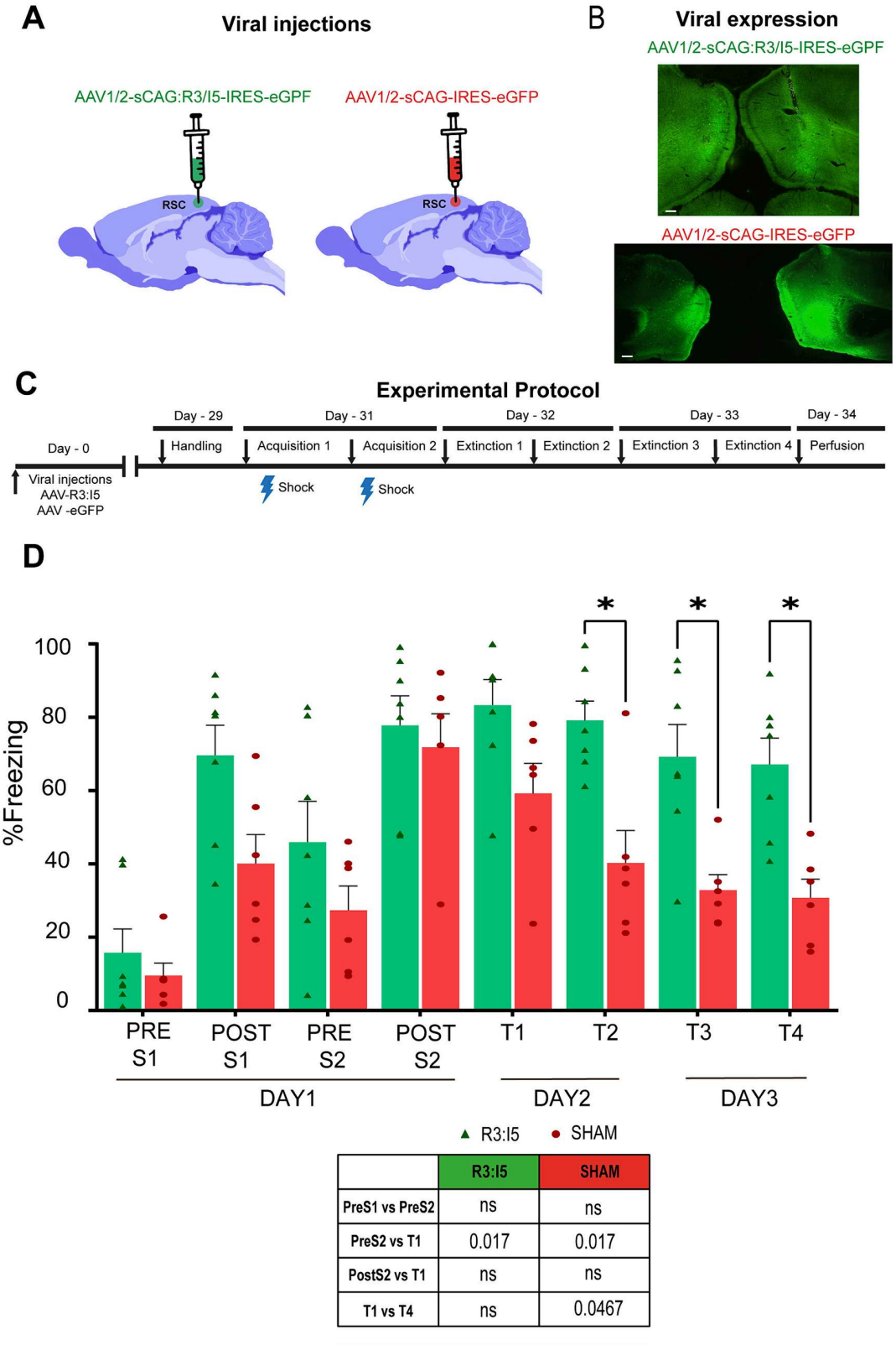

	R3:I5	SHAM
PreS1 vs PreS2	ns	ns
PreS2 vs T1	0.017	0.017
PostS2 vs T1	ns	ns
T1 vs T4	ns	0.0467

Fig. 1. Effect of chronic RXFP3 activation by R3/I5 on contextual fear memory. (A) Schematic of the surgical procedure illustrating the injection into the RSC of AAV1/2-sCAG:R3/I5-IRES-eGFP (R3/I5 group; left) or AAV-sCAG-IRES-eGFP (control SHAM group; right). (B) Illustration of eGFP fluorescence associated with the bilateral expression of the R3/I5 AAV (upper) and the control AAV (lower). Scale bar 200 μm. (C) Schematic timeline of the various procedures conducted during the behavioral protocol. (D) Comparison of freezing levels observed in R3/I5 group rats (green; n = 7) and control SHAM group rats (red; n = 7).

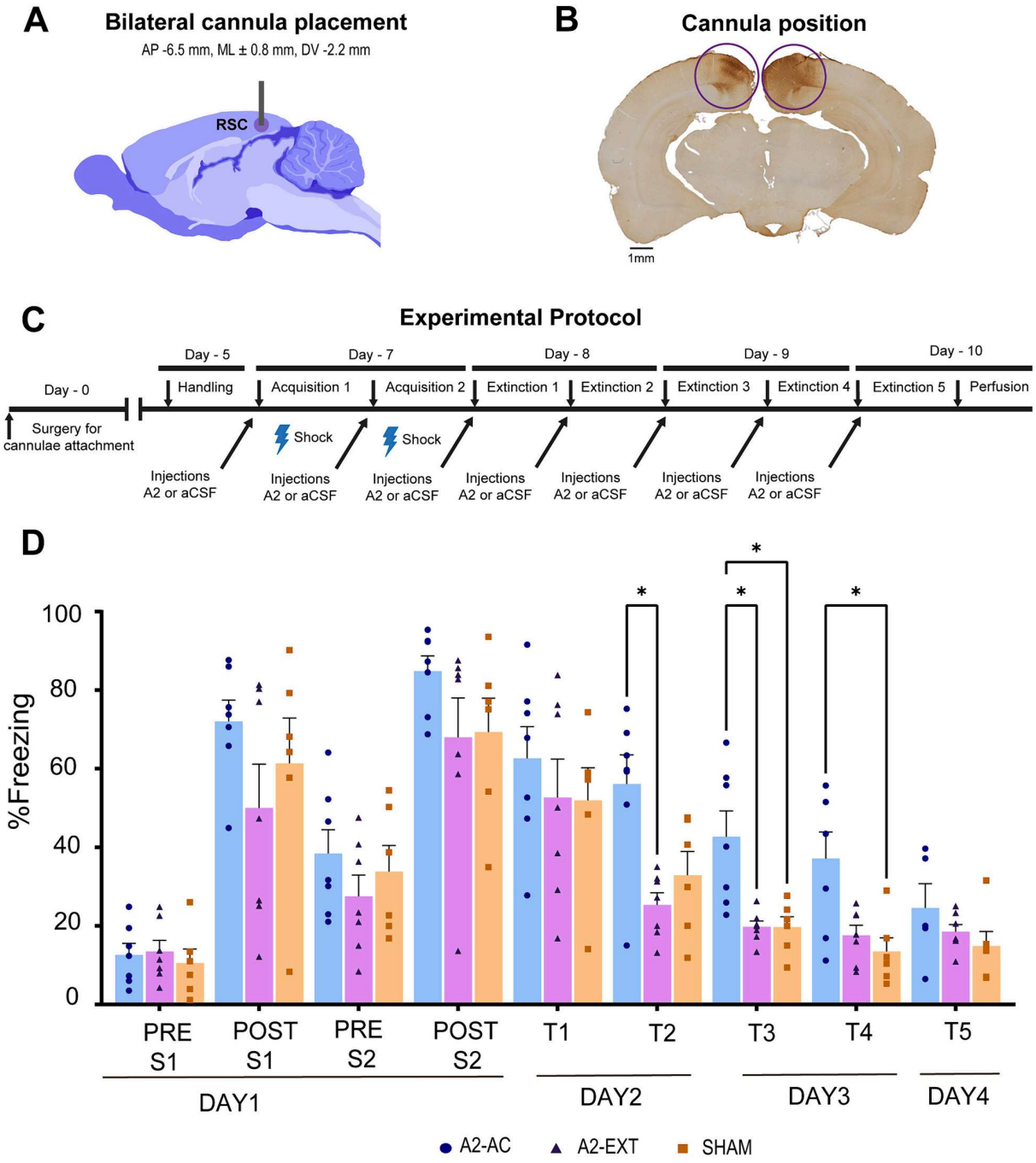

	A2- AC	A2- EXT	SHAM
PreS1 vs PreS2	ns	ns	ns
PreS2 vs T1	ns	ns	ns
PostS2 vs T1	ns	ns	ns
T1 vs T4	ns	0.035	0.05

Fig. 2. Effect of acute RXFP3 activation by A2 on contextual fear memory. (A) Schematic of the surgical procedure illustrating the coordinates of the guide cannula placement in the RSC. (B) Illustration of a histological coronal brain section indicating the position of the bilateral indwelling cannulae (circled). Scale bar 1 mm. (C) Schematic timeline of the various procedures conducted during the behavioral protocol. (D) Comparison of freezing levels observed in rats receiving a bilateral A2 injection 15 min prior to the acquisition sessions (A2-AC; blue; n = 8); or 15 min prior to the extinction sessions (A2-EXT; purple; n = 8) and in rats receiving aCSF 15 prior to all sessions (SHAM; orange; n = 8).

classification and quantification of elements in images. It works by identifying and classifying each object based on a set of predefined measurements, such as marker intensity, shape, or size. In our study, this feature was utilized to efficiently differentiate and count neurons exhibiting RXFP3, vGLUT1, and vGAT mRNA. Adjustments to the classifier's parameters were made to recognize the unique characteristics of these neurons. Importantly, the parameters were kept consistent across all animals and ROIs to ensure uniformity in data analysis. This approach enabled a more accurate and detailed quantification of neuronal co-localization in the regions of interest.

2.8. Data analyses

Measures obtained were plotted as percentages in a database of the statistical program GraphPad Prism 9 (GraphPad Software Inc., LaJolla, CA, USA). Normality Shapiro-Wilk and Kolmogorov-Smirnov tests were applied to assess the normal distribution of data in each sample.

Two-way ANOVAs were performed, followed by Bonferroni and Tukey post-hoc analyses. The α value was set at 0.05 for all analyses.

3. Results

3.1. Impact of chronic and acute RXFP3 activation in RSC on contextual fear conditioning

In experiments to determine the effect of RLN3/RXFP3 signalling in the RSC on contextual fear, we initially injected AAV bilaterally into the RSC, which produced and secreted locally the RXFP3 agonist peptide, R3/I5 [35,36], to assess the effect of chronic local RXFP3 activation on the conditioning process. In subsequent studies to dissect the nature of the overall effects observed, we injected the selective RXFP3 agonist peptide, A2 [37], into the RSC just prior to each acquisition, or (retrieval)/extinction session to assess the effect of acute RXFP3 activation on these specific processes.

3.1.1. Effect of chronic RXFP3 activation by R3/I5 on contextual fear memory

A two-way repeated measures ANOVA between and within groups (SHAM, n = 7; R3/I5, n = 7) was conducted with one grouping variable (treatment) and one repeated measure (conditioning sessions). The main effects of the conditioning session was significant [$F(2.878, 31.66) = 18.81$, $p < 0.001$], as was the main treatment effects [$F(1, 11) = 14.08$, $p = 0.0032$].

Post-hoc analysis with Sídák's multiple comparisons test indicated that during the last three extinction sessions (T2, T3 and T4) SHAM rats displayed significantly less freezing than R3/I5 treated rats (T2, $p = 0.0393$; T3, $p = 0.0410$; T4, $p = 0.0152$). Although the SHAM group displayed less freezing during PostS2 than the R3/I5 group, this difference was not significant, and no other comparisons between treatments were significant.

Acquisition of conditioned responses was examined by measuring freezing in sessions PreS1, PreS2, PostS2 and T1.

Both groups of rats displayed equivalent levels of freezing during the pre-shock time of the first acquisition session (PreS1) and the second acquisition session (PreS2) (R3/I5, $p = 0.3410$; SHAM, $p = 0.2256$). Furthermore, before the shock in the second conditioning session (PreS2), both groups froze less than during the first extinction session (T1; $p = 0.0170$, for both groups), indicating the acquisition of fear conditioning. No differences were detected in the level of freezing between PostS2 and T1 in either group (Fig. 1).

Extinction was assessed by testing for differences in the level of freezing by the rats in both groups between the T1 and T4 sessions. Rats in the R3/I5 group did not display significant differences in freezing between these two sessions ($p = 0.7984$), while rats in the control SHAM group displayed a significant reduction in freezing between the first and last extinction session ($p = 0.0467$; Fig. 1). These data indicate an impairment in the extinction of context-conditioned fear in the R3/I5 treated rats, due to the continuous bilateral activation of RXFP3 in the RSC.

3.1.2. Pre-acquisition RXFP3 activation inhibited extinction of contextual fear memory

In order to assess whether the effect observed with the chronic activation of RXFP3 in the RSC was associated with the acquisition and/or extinction process, we employed an acute pharmacological approach in three groups of rats that received bilateral injections into the RSC of either: the RXFP3 agonist, A2, before each acquisition session and aCSF before each extinction session (A2-AC, n = 8); or A2 before each extinction session and aCSF before each acquisition session (A2-EXT, n = 8); or aCSF before each acquisition and extinction session (SHAM, n = 8).

A two-way repeated measures ANOVA between and within groups was conducted with one grouping variable (treatment) and one repeated measure (conditioning sessions). The main effects of the conditioning session were significant [$F(4.107, 86.25) = 42.38$, $p < 0.001$], as was the main subject effects [$F(21,147) = 6.297$, $p < 0.001$].

Post-hoc analysis with Tukey's multiple comparisons test indicated that rats that received RXFP3 agonist prior to the acquisition sessions (A2-AC) displayed significantly more freezing in extinction sessions 2 and 3 than rats that received aCSF prior to acquisition and RXFP3 agonist prior to the extinction sessions (A2-EXT) (T2, $p = 0.0393$; T3, $p = 0.0410$). Rats in the A2-AC group also displayed significantly more freezing in extinction sessions 3 and 4 than rats in the SHAM group (T3, $p = 0.0393$; T4, $p = 0.0410$), but no other comparisons between treatments were significant.

Acquisition of conditioned responses was examined by measuring freezing in sessions PreS1, PreS2, Post2 and T1. All groups displayed equivalent levels of freezing during the pre-shock time of the first acquisition session (PreS1) and the second acquisition session (PreS2) (A2-AC, $p = 0.0667$; A2-EXT, $p = 0.1184$; SHAM, $p = 0.0797$). Both groups of rats froze less before the shock in the second conditioning session (PreS2) than during the first extinction session (T1) (A2-AC, $p = 0.3904$; A2-EXT, $p = 0.3207$; SHAM, $p = 0.7986$), which indicated the acquisition of fear conditioning. No differences were detected in the level of freezing between PostS2 and T1 in either group (Fig. 2).

Extinction was assessed by testing for differences in the level of freezing by the rats in both groups between the T1 and T4 sessions. Rats in the A2-AC group did not display significant differences between these two sessions ($p = 0.1956$), while rats in the A2-EXT and SHAM groups displayed significant differences between the first and last extinction session (A2-EXT, $p = 0.0350$; SHAM, $p = 0.05$; Fig. 2). These data indicate an impairment in the extinction of context-conditioned fear in the A2-AC group of rats due to the acute bilateral activation of RXFP3 in the RSC.

3.2. Expression of RXFP3 mRNA in GABAergic and glutamatergic neurons of RSC

For the delineation of the divisions and subdivisions of the RSC we used established cytoarchitectonic criteria [44]. In brief, we divided the RSC into an agranular A30 and granular A29 area according to the granular layer V in A29 and the neuronal density in layers II/III, also in A29. We also subdivided the A29 area into three subareas A29a, A29b and A29c. A29a is the ventral area where delineation of layers is difficult as there appears to be a uniform layer. A29b is vertical in coronal sections and layers II/III contain a thin layer II and a wider layer III. A29c appears more dorsally and is characterized by an arrangement of layer III neurons in rows parallel to the pial surface. RLN3 immunoreactivity was present in a high density of fibers throughout the extent of the RSC (Fig. 3). Fibers innervating the RSC arrive via the subicular area and enter A29c of the RSC. Although RLN3 positive nerve fibers were observed in all layers, layer V contained the highest density, particularly

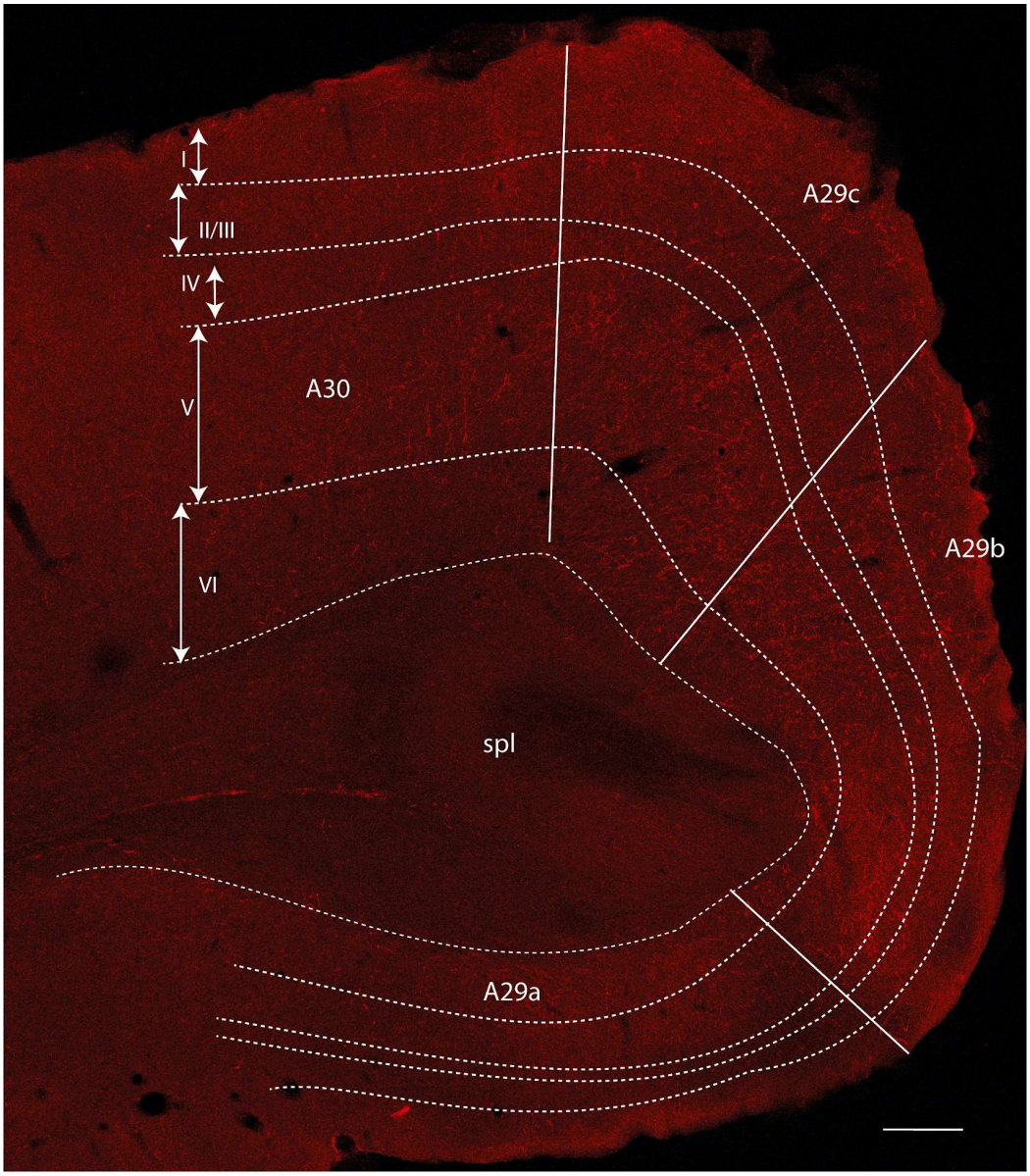

Fig. 3. Confocal image of immunofluorescent RLN3 immunoreactivity in a coronal section through the unilateral RSC. RLN3-positive fibers were particularly concentrated in layer V, but dispersed fibers were observed in all layers. Calibration bar 200 μm.

in A29b (Fig. 3).

A multiplex *in situ* hybridization (RNAscope™) study was performed to estimate the relative proportion of glutamatergic and GABAergic RSC neurons that express RXFP3 mRNA. A separate analysis was conducted for the A30 and A29 areas and for the A29a, A29b and A29c fields. DAPI fluorescence was used to discriminate between RSC layers I-VI. We analyzed data from the RSC of four naïve rat brains, but as there was considerable variability in the absolute numbers of neurons labeled in different brains, a formal statistical analysis was not undertaken. However, the relative proportions of single-, double-, and triple-labeling were similar between cases. Thus, we analyzed the relative proportions of vesicular GABA transporter (vGAT), vesicular glutamate transporter-1 (vGLUT1) and RXFP3 mRNA co-labeling observed in A30 and A29a-c in a single RSC (Figs. 4-7).

DAPI labeling allowed the discrimination of single-, double- or triple-labeling in different cortical layers of the A30 area (Fig. 4A). In general, RXFP3 mRNA was more frequently expressed in neurons containing vGAT mRNA than in those containing vGLUT1 mRNA in layers I to V (Fig. 4B-E). However, notably, in layer VI, the situation was reversed (Fig. 4F). Nonetheless, the absolute number of vGLUT1 mRNA labeled cells in layer VI, was much lower than in the upper layers. Notably, the most RXFP3 mRNA-labeled neurons occurred in upper layer I (Fig. 4B) and layers II/III (Fig. 4C).

Analysis of the co-expression of RXFP3 mRNA with vGLUT1 or vGAT mRNA in subregion A29c, revealed a strong association of RXFP3 and vGAT mRNA. vGAT mRNA was relatively abundant, while vGLUT1 mRNA was only apparent at higher magnification in layers II/III (Fig. 5A). In layer I, there was a lower density of neurons and there was higher number of RXFP3/vGAT mRNA double-labeled neurons than RXFP3/vGLUT1 mRNA labeled cells (Fig. 5B). Layers II/III were characterized by densely packed vGLUT1 mRNA-positive neurons. However, the proportion of vGAT/RXFP3 mRNA co-expression was higher than that of vGLUT1/RXFP3 mRNA co-expression (Fig. 5C). Layer IV was narrower than the other layers and displayed a low cell density. In this

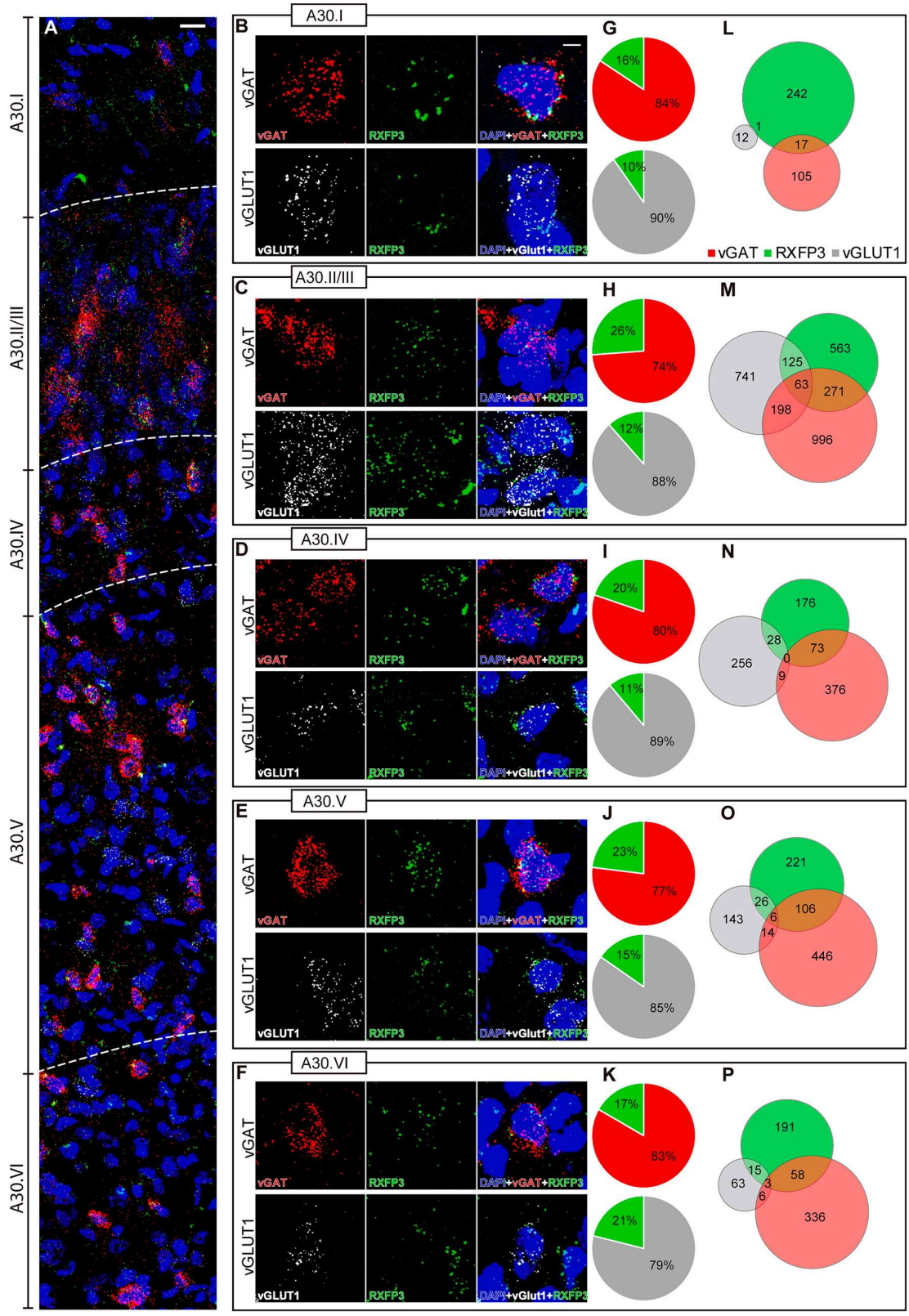

Fig. 4. Comparative distribution of RXFP3 mRNA-positive neurons within different layers of A30 revealed by specific probes for RXFP3 (green), vGLUT1 (white) and vGAT (red) mRNA and counterstained with DAPI. (A). Overview of the layers and their boundaries along a vertical strip of A30. Calibration bar 20 μm. (B-F) Single and double labeling for cells in different layers of A30. Calibration bar 5 μm. (G-K) Pie charts illustrating the proportion of vGAT neurons (red) vGLUT1 neurons (grey) that express RXFP3 (green) mRNA. (L-P) Venn diagrams illustrating the number of single-, double- or triple-labeled neurons for each probe.

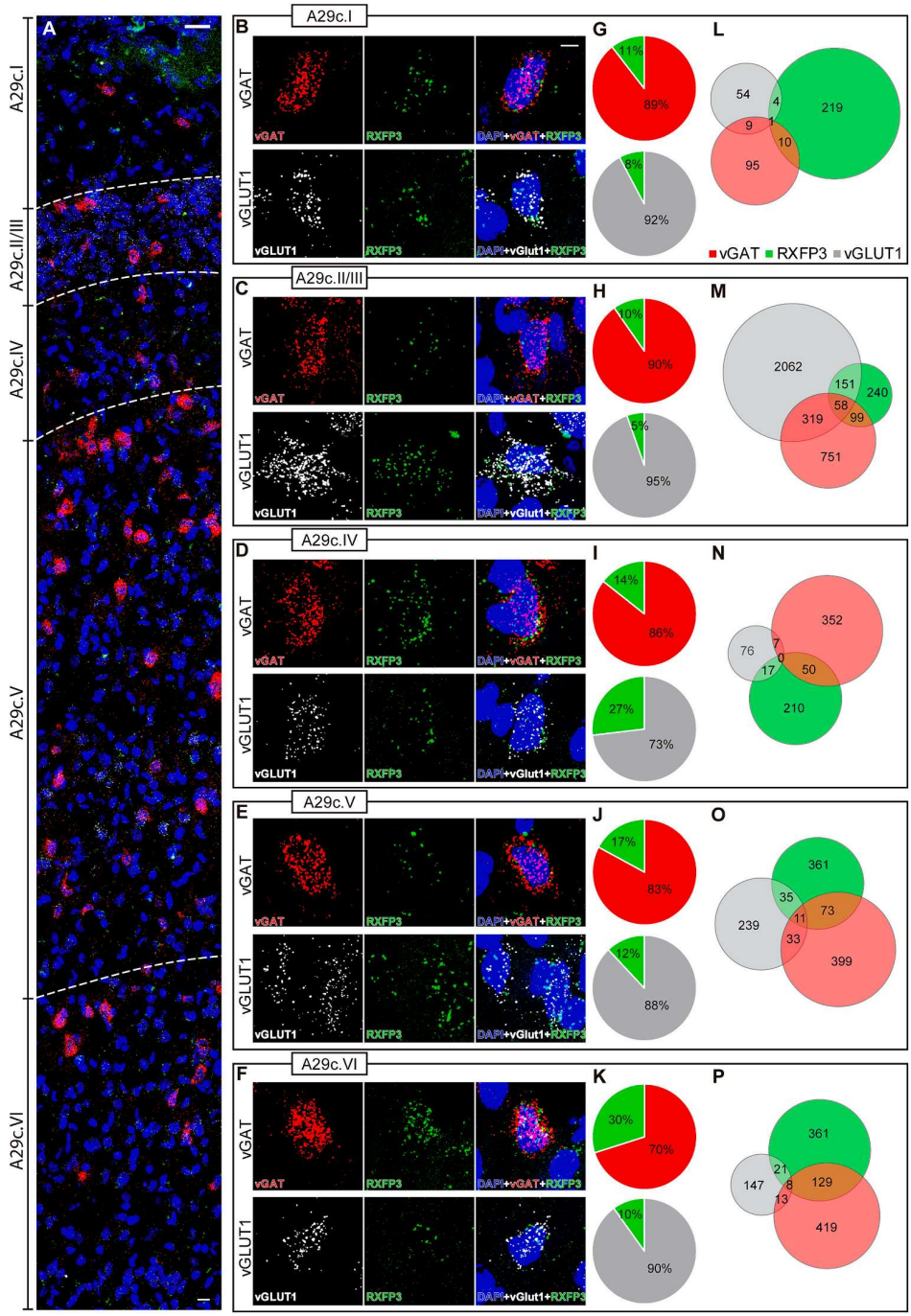

Fig. 5. Comparative distribution of RXFP3 mRNA-positive neurons within different layers of A29c revealed by specific probes for RXFP3 (green), vGLUT1 (white) and vGAT (red) mRNA and counterstained with DAPI. (A). Overview of the layers and their boundaries along a vertical strip of A29c. Calibration bar 20 μm. (B-F) Single and double labeling for cells in different layers of A29c. Calibration bar 5 μm. (G-K) Pie charts illustrating the proportion of vGAT neurons (red) vGLUT1 neurons (grey) that express RXFP3 (green) mRNA. (L-P) Venn diagrams illustrating the number of single-, double- or triple-labeled neurons for each probe.

layer, the number of vGLUT1 mRNA positive neurons was very low but many of these expressed RXFP3 mRNA (Fig. 5D). In contrast, the absolute number of vGAT neurons was higher in layer IV and the proportion of RXFP3/vGAT mRNA co-expressing cells was increased over that in the upper layers. In layer V, the absolute number and proportion of vGAT mRNA positive neurons and vGAT/RXFP3 mRNA labeled cells was higher than the absolute number and proportion of vGLUT1/RXFP3 mRNA cells (Fig. 5E). Finally, the polymorphic layer VI also contained a higher proportion of vGAT/RXFP3 mRNA neurons than vGLUT1/RXFP3 mRNA neurons (Fig. 5F).

In the A29b field, there was a generally stronger association of RXFP3 mRNA with vGAT mRNA than with vGLUT1 mRNA (Fig. 6). Area 29b displayed a dense layer II/III composed mainly of vGLUT1 mRNA positive neurons (Fig. 6A). In layer I, there was a considerable number of RXFP3 mRNA positive cells, but very few displayed either vGLUT1 or vGAT mRNA (Fig. 6B). In contrast, layers II/III contained a high density of vGLUT1 mRNA positive neurons, but the percentage of vGAT/RXFP3 mRNA double-labeled neurons was higher than the percentage of

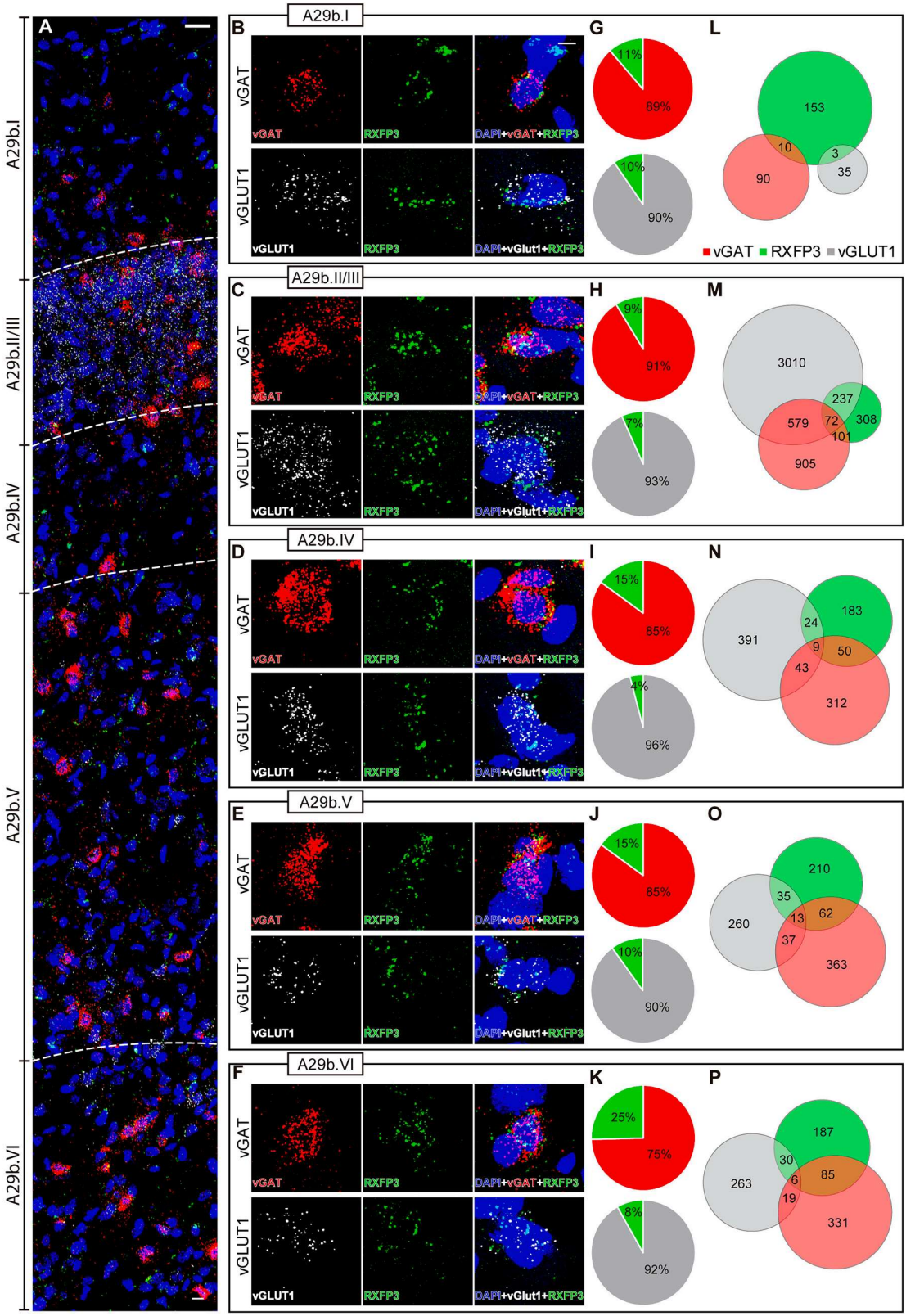

Fig. 6. Comparative distribution of RXFP3 mRNA-positive neurons within different layers of A29b revealed by specific probes for RXFP3 (green), vGLUT1 (white) and vGAT (red) mRNA and counterstained with DAPI. (A). Overview of the layers and their boundaries along a vertical strip of A29b. Calibration bar 20 μm. (B-F) Single and double labeling for cells in different layers of A29b. Calibration bar 5 μm. (G-K) Pie charts illustrating the proportion of vGAT neurons (red) vGLUT1 neurons (grey) that express RXFP3 (green) mRNA. (L-P) Venn diagrams illustrating the number of single-, double- or triple-labeled neurons for each probe.

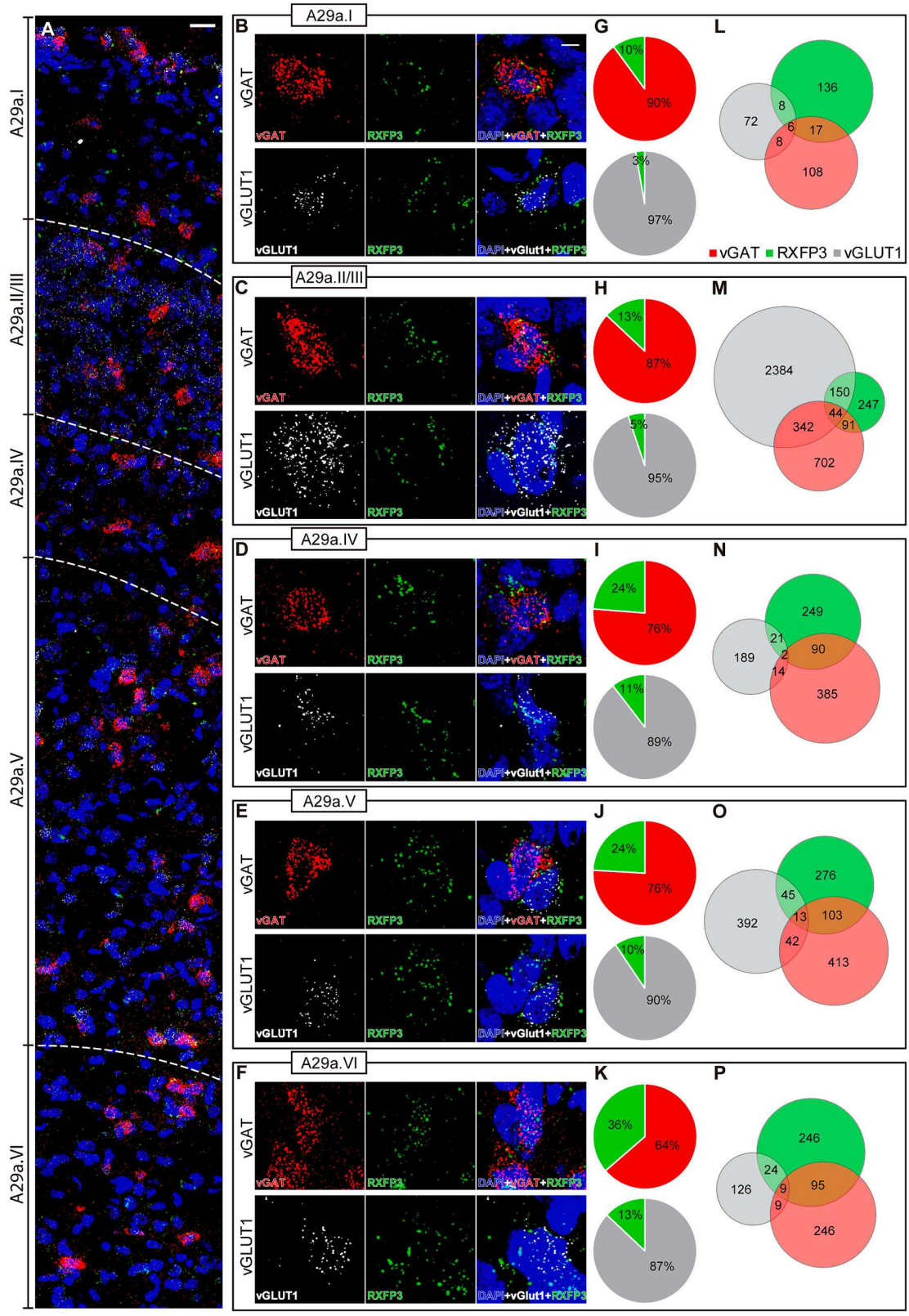

Fig. 7. Comparative distribution of RXFP3 mRNA-positive neurons within different layers of A29a revealed by specific probes for RXFP3 (green), vGLUT1 (white) and vGAT (red) mRNA and counterstained with DAPI. (A). Overview of the layers and their boundaries along a vertical strip of A29a. Calibration bar 20 μm. (B-F) Single and double labeling for cells in different layers of A29a. Calibration bar 5 μm. (G-K) Pie charts illustrating the proportion of vGAT neurons (red) vGLUT1 neurons (grey) that express RXFP3 (green) mRNA. (L-P) Venn diagrams illustrating the number of single-, double- or triple-labeled neurons for each probe.

vGLUT1/RXFP3 mRNA labeled cells (Fig. 6C). Layer IV contained a similar number of vGLUT1 mRNA and vGAT mRNA neurons and the proportion of vGAT/RXFP3 mRNA double-labeling was higher than the proportion of vGLUT1/RXFP3 mRNA double-labeling (Fig. 6D). A similar situation was observed in layer V (Fig. 6E) and layer VI (Fig. 6F). In addition, nearly 30 % of vGAT mRNA neurons in layer VI were RXFP3 mRNA positive.

In area 29a, the relative proportions of vGAT/RXFP3 mRNA and vGLUT1/RXFP3 mRNA co-expression was more different than in other RSC subfields (Fig. 7). In this area it was difficult to differentiate between the cortical layers apart from layer I (Fig. 7A). In layer I, most labeled cells displayed RXFP3 mRNA signal and the proportion of vGAT/RXFP3 mRNA double-labeling was greater than that for vGLUT1/RXFP3 mRNA (Fig. 7B) This difference increased in the deeper, inner layers of the RSC. In layers II/III, although the number of vGLUT1 mRNA neurons was three times the number of vGAT mRNA neurons, the percentage of vGLUT1/RXFP3 mRNA cells was only 5 % of the total vGLUT1 mRNA cells, while the proportion of vGAT/RXFP3 mRNA double-labeled neurons was 13 % of the total vGAT mRNA cells (Fig. 7C). Neurons in layer IV were loosely packed and the number of vGAT mRNA cells was higher than the number of vGLUT1 mRNA cells. Again, the percentage of vGAT/RXFP3 mRNA co-expression was 24 % of the total vGAT mRNA cells, and 11 % of the total vGLUT1 mRNA cells co-expressed vGLUT1/RXFP3 mRNA (Fig. 7D). An identical proportion of labeling was observed in the wider layer V, where vGAT/RXFP3 mRNA was detected in 24 % of vGAT mRNA cells, with vGLUT1/RXFP3 mRNA co-expression detected in 10 % of the total vGLUT1 mRNA cells (Fig. 7E). The largest difference was observed in layer VI where the percentage of vGAT/RXFP3 and vGLUT1/RXFP3 mRNA positive cells accounted for 36 % and 13 % of the respective total number of vGAT and vGLUT1 mRNA positive neurons (Fig. 7F).

A quantitative analysis of the different layers and areas of the RSC revealed that, despite a higher abundance of glutamatergic neurons (22.1 %) than GABAergic neurons (16.4 %) throughout the RSC, the proportion of RXFP3-positive vGAT neurons (3.2 %) was greater than that of RXFP3-positive glutamatergic neurons (2 %).

Examination of the RSC granular layer (A29a, A29b, A29c) and agranular layer (A30) revealed similar average percentages of RXFP3 mRNA-positive neurons present in each (9.6 % and 10.2 %, respectively), with a vGAT mRNA-positive population of 16.4 % and 16.6 %, respectively, and a different percentage of vGLUT1 mRNA-positive neurons (27.1 % and 8.9 %, respectively). Furthermore, we observed similar percentages of RXFP3 mRNA and vGAT mRNA positive neurons across the four areas (A29a 9.6 % and 15.4 %; A29b 9.3 % and 17.8 %; A29c 9.7 % and 16 %; A30 10.2 % and 16.6 %), while the percentages of vGLUT1 mRNA positive neurons displayed greater variability (A29a 26.3 %; A29b 35.3 %; A29c 20.4 %; A30 8.9 %). The neuronal density of RXFP3/vGLUT1 mRNA-positive neurons was lower in all areas of the granular layer (A29a 7.9 %; A29b 8.3 %; A29c 8.9 %) than in the agranular layer (A30 16.1 %). By comparison, the co-expression of RXFP3/vGAT mRNA was higher in A29a (21.3 %) and A30 (23.2 %) than in A29b (15.3 %) and A29c (17.9 %).

4. Discussion

This pharmacological study suggests a modulatory effect of RLN3 on context-conditioned fear processes via activation of RXFP3 receptors on inhibitory GABAergic interneurons, this effect being observed both chronically after administration of the R3/I5 viral particle and acutely after injection of the RXFP3 agonist, A2, into the RSC.

Activation of RXFP3 in the RSC may be involved in the initial formation of fear associations with context, as administration of A2 prior to acquisition but not prior to extinction was observed to impair the extinction process of fear memories. It can also be inferred that activation of RXFP3 in the RSC interferes with the arousal-inhibition balance, leading to a delay in the extinction process of contextual fear conditioning.

Regarding the expression of RXFP3, vGLUT1 and vGAT mRNA in the RSC, we found consistent levels of RXFP3 mRNA and vGAT mRNA-positive neurons in all four areas of the RSC, with varying percentages of vGLUT1 mRNA-positive neurons. The neuronal density of RXFP3/vGLUT1 mRNA-positive neurons was lower in the granular layer compared with the agranular layer. In addition, RXFP3/vGAT mRNA coexpression was higher in A29a and A30 than in A29b and A29c. Notably, a higher proportion of GABA + RXFP3 neurons compared to vGLUT1 + RXFP3 neurons was observed in all layers and areas of the RSC.

The occurrence of RXFP3 in GABAergic neurons has been shown in the septum where RXFP3 is associated with parvalbumin neurons [45], the hippocampus, where it is associated with somatostatin expressing neurons [36] and in the amygdala where some RXFP3 and vGAT neurons also express somatostatin [42]. It has also been documented that RLN3 fibers are associated with calcium binding protein expressing neurons in the amygdala and septum [46,47]. We have also observed RXFP3 expression in vGLUT1 RSC neurons but the exact role and relevance to behavior have not been studied.

The role of the RSC in context conditioning processing is to involve the convergent inputs of sensory internal and external stimuli and bidirectional projections with the hippocampal formation [6,10,48]. Our data indicate that acquisition and extinction of context conditioning are related, not independent, processes. Relative to cued fear conditioning, the acquisition and within session extinction processes are dependent on the lateral amygdala, but the recall of the extinction process the next day involves the infralimbic cortex [49,50]. In contrast, it has been reported that lesion of the RSC before acquisition only has small effects on the codification and retrieval of contextual fear conditioning, while a major impairment occurs when the RSC lesion is made after acquisition [9,51]. It can be argued that the lack of effect of the pretraining RSC lesion is due to the use of alternative pathways to configure the acquisition process, while after the post-training RSC lesion, the natural pathway of memory retrieval is damaged. Our results indicate that acquisition of contextual fear conditioning is being achieved under different conditions than for cued fear conditioning. Following an inhibitory pharmacological action on RXFP3 expressing neurons in the RSC, we did not observe changes in the acquisition or retrieval of contextual conditioning, but instead, a slowing of extinction mediated by RXFP3 activation in the RSC. Thus, in the presence of an RXFP3 agonist, the ‘plastic’ neural changes occurring in the RSC make the subsequent re-exposure to the context without US more refractory to extinction.

On the basis of previous studies of RXFP3-related cell signalling and neuronal responses in cell-based systems, brain slices and *in vivo*, the presence of exogenous RXFP3 agonist within the neuropil of the RSC during the acquisition/extinction process may activate three signalling processes within specific RXFP3-positive neurons in the RSC, namely: (i) a rapid mechanism of increased inhibition via ion channel-associated currents (M−current) [52], (ii) sustained inhibition of a AC/cAMP cascade [29], and (iii) activation of the ERK1/2 cascade [31,32]. Moreover, to decipher the precise role of these possible cellular mechanisms in relation to the observed behavioral outcomes, it is important to consider that RXFP3 mRNA expression was more prominent in vGAT mRNA positive neurons than in vGLUT1 mRNA positive neurons in the RSC. Thus, RXFP3 activation would likely have a greater effect on inhibitory, GABAergic than excitatory, glutamatergic neurons. Furthermore, previous studies in rats and mice suggest that the population of GABAergic neurons involved might be somatostatin-expressing neurons [27,36].

Regarding the possible rapid inhibition of RXFP3-expressing neurons in the RSC, RXFP3 activation in the paraventricular hypothalamic nucleus produced an inhibitory effect on hypothalamic oxytocin (and arginine vasopressin) neurons by activating an M−like K^+ current [53]. This current was a voltage-dependent, slowly activating and non-

inactivating K^+ conductance which contributes to the resting potential membrane and is involved in the regulation of excitability [54]. The outward current produced by RXFP3 activation was dependent on a Ca^{2+} conductance, as it was attenuated by Cd^{2+}, a potent Ca^{2+} channel blocker [52]. Thus, as a higher level of RXFP3 mRNA expression was observed in inhibitory GABAergic neurons in the RSC, RXFP3-mediated inhibition of these neurons may result in increased glutamatergic neuron output responses within the region.

Regarding the effect of acute or chronic RXFP3 activation on cAMP signalling pathways, in Chinese hamster ovary (CHO) cells expressing RXFP3, RLN3 blocked the increase in cAMP obtained by application of forskolin [29]. Notably, the AC/cAMP pathway has been established as a key pathway for memory acquisition and consolidation in a fear conditioning paradigm via the consecutive activation of protein kinase A (PKA) and the cAMP-responsive element binding protein (CREB), which activates key memory-associated genes [55,56]. CREB phosphorylation, produced by PKA activation, is one of the long-term mechanisms associated with different forms of conditioned learning and extinction in the amygdala and the hippocampus, depending on the nature of the cued or contextual conditioning, respectively [57]. Moreover, persistence of extinction memory to a cue is also dependent on cAMP regulated pathways in the infralimbic cortex [58]. Specifically, extinction of contextual fear required down-regulation of the cAMP-PKA-CREB pathway in the RSC [59]. Considering this, the inhibition of the pathway through phosphodiesterase activation may not inhibit extinction unless this mechanism be restricted to inhibitory neurons such as vGAT neurons expressing RXFP3.

A further intracellular signalling mechanism that can be triggered by RXFP3 activation is the ERK1/2 cascade pathway. This activation was first described in CHO and HEK cells [31] and later altered levels of pERK were observed in the septum [32] and amygdala [42] following the intracerebroventricular (icv) injection of an RXFP3 agonist, although these latter effects may have been indirect. Notably, a role for ERK activation in the plasticity mechanisms induced by extinction of trace conditioning has been described in the RSC [13]. Additionally, under certain conditions in the hippocampus, resistance to context conditioning extinction has been shown to be dependent on ERK-mediated coactivation of NR2A and NR2B subunits of NMDA receptors [60]. Additional studies would be necessary to obtain data on the specific role of inhibitory interneurons of the RSC in processing acquisition or extinction and quantification of the variations of key downstream signalling along this process is necessary to assess the mechanisms mechanism triggered by RXFP3 activation.

Previous studies have reported a role of the RLN3/RXFP3 signalling system in different aspects of the learning and memory processes [61]. These works have been focused on the septo-hippocampal system for spatial memory tasks and on the amygdala-prefrontal cortex for emotional related processes. In the present work, we claim for a special participation of the RLN3-RXFP3 system in the contextual fear extinction through the RSC. It is worth noting that, in spite the main effect that emerges during the extinction process, the step that is mainly affected is acquisition. This may be one of the most important differences with the cued acquisition/extinction processes. In cued conditioning the memory is acquired in the amygdala whereas the extinction memory is stored and retrieved in the infralimbic prefrontal cortex [49]. Also, the extinction memory is contextual dependent as appears in the reinstatement process [62]. Thus, a transfer should occur between the RSC and the prefrontal cortex. In fact, such kind of transfer has been described for the contextual engrams [63].

In transgenic mice expressing cre under the promotor of RLN3, it has been shown that long telencephalic RLN3 projections to the RSC comes from the NI in the pontine tegmentum [22]. Unpublished data from our lab on both retrograde and anterograde tracers also confirm that the main source of RLN3 afferents to the RSC arises from the NI. We have also observed that projections from the NI to the medial septum and different areas of the temporal lobe including entorhinal cortices and hippocampus comes from different subsets of neurons displaying a low level of collateralization. Thus, it is expected that projections to the RSC also comes from an independent set of NI neurons. The action of the NI and its associated RLN3/RXFP3 signalling system could be also related to the contribution of the hippocampus to the contextual fear conditioning. The activity of NI innervation on somatostatin neurons in the CA1 field disrupts the acquisition of contextual fear conditioning [27] and CA1 is one of the main afferents to the A29 RSC. Thus, both processes, the acquisition on CA1 field and the extinction on RSC may be to linked processes both directed from the NI.

In conclusion, we have demonstrated that activation of RXFP3 in the RSC delays contextual fear extinction, but the main impact of this activity occurs during acquisition by inhibiting inhibitory interneurons. Long term actions of the RLN3/RXFP3 system on the RSC in contextual fear conditioning has not been analysed yet, but persistence of fear to unpredictable cues like the context could be considered a feature of a post-traumatic stress disorder (PTSD) syndrome and there is abundant literature on the role of RLN3 in anxiety processes [36,64].

Funding

This research was funded by the UJI predoctoral program PREDOC/2021/19 (MN-S), the UJI postdoctoral program POSDOC/2021/19 (IG-M); Fundación Alicia Koplowitz, Spain, grant number 19I436 (FEO-B, EC-G); the Spanish Ministerio de Ciencia, Innovación y Universidades, grant number RTI2018-095698-B-I00 (FEO-B, IG-M, EC-G); AICO Generalitat Valenciana, grant number AICO/2021/246 (EC-G, FEO-B), the Plan Nacional sobre Drogas of the Spanish Ministerio de Sanidad y Consumo grant number 2020I012 (FEO-B and EC-G) and UJI-B2019-54 (FEO-B). Studies at the Florey Institute were supported by the Victorian Government's Operational Infrastructure Support Program.

CRediT authorship contribution statement

Mónica Navarro-Sánchez: Writing – review & editing, Writing – original draft, Visualization, Methodology, Investigation, Formal analysis, Data curation, Conceptualization. **Isis Gil-Miravet:** Writing – review & editing, Writing – original draft, Visualization, Supervision, Methodology, Investigation, Formal analysis, Data curation, Conceptualization. **Daniel Montero-Caballero:** Writing – review & editing, Investigation, Formal analysis, Data curation. **Ross A.D. Bathgate:** Writing – review & editing, Resources, Methodology. **Mohammed Akhter Hossain:** Writing – review & editing, Resources. **Esther Castillo-Gómez:** Writing – review & editing, Supervision, Funding acquisition, Formal analysis, Data curation, Conceptualization. **Andrew L. Gundlach:** Writing – review & editing, Writing – original draft, Visualization, Formal analysis. **Francisco E. Olucha-Bordonau:** Writing – review & editing, Writing – original draft, Visualization, Validation, Supervision, Project administration, Methodology, Funding acquisition, Formal analysis, Data curation, Conceptualization.

Declaration of competing interest

The authors declare that they have no known competing financial interests or personal relationships that could have appeared to influence the work reported in this paper.

Data availability

Data will be made available on request.

Acknowledgements

Supported by Red Española de Investigación en Estrés/Spanish Network for Stress Research RED2022-134191-T financed by MCIN/AEI /10.13039/501100011033. We are indebted to the confocal facility and

animal facility (SEA) of the Servicio Central de Instrumentación Científica (SCIC) of UJI and Victoria Ibáñez from the Statistics Department UJI.

References

[1] A. Maass, S. Landau, A. Horng, S.N. Lockhart, G.D. Rabinovici, W.J. Jagust, S. L. Baker, R. La Joie, Comparison of multiple tau-PET measures as biomarkers in aging and Alzheimer's disease, Neuroimage 157 (2017) 448–463, https://doi.org/10.1016/j.neuroimage.2017.05.058.

[2] C.R. Jack, H.J. Wiste, C.G. Schwarz, V.J. Lowe, M.L. Senjem, P. Vemuri, S. D. Weigand, T.M. Therneau, D.S. Knopman, J.L. Gunter, D.T. Jones, J. Graff-Radford, K. Kantarci, R.O. Roberts, M.M. Mielke, M.M. MacHulda, R.C. Petersen, Longitudinal tau PET in ageing and Alzheimer's disease, Brain 141 (2018) 1517–1528, https://doi.org/10.1093/brain/awy059.

[3] E. Valenstein, D. Bowers, M. Verfaellie, K.M. Heilman, A. Day, R.T. Watson, Retrosplenial amnesia, Brain 110 (1987) 1631–1646, https://doi.org/10.1093/brain/110.6.1631.

[4] J.P. Aggleton, Understanding retrosplenial amnesia: insights from animal studies, Neuropsychologia 48 (2010) 2328–2338, https://doi.org/10.1016/j.neuropsychologia.2009.09.030.

[5] S.D. Vann, J.P. Aggleton, E.A. Maguire, What does the retrosplenial cortex do? Nat. Rev. Neurosci. 10 (2009) 792–802, https://doi.org/10.1038/nrn2733.

[6] A.F. De Sousa, K.K. Cowansage, I. Zutshi, L.M. Cardozo, E.J. Yoo, S. Leutgeb, M. Mayford, Optogenetic reactivation of memory ensembles in the retrosplenial cortex induces systems consolidation, Proc. Natl. Acad. Sci. (USA) 116 (2019) 8576–8581, https://doi.org/10.1073/PNAS.1818432116.

[7] K.K. Tayler, K.Z. Tanaka, L.G. Reijmers, B.J. Wiltgen, Reactivation of neural ensembles during the retrieval of recent and remote memory, Curr. Biol. 23 (2013) 99–106, https://doi.org/10.1016/j.cub.2012.11.019.

[8] K.A. Corcoran, N. Yamawaki, K. Leaderbrand, J. Radulovic, Role of retrosplenial cortex in processing stress-related context memories, Behav. Neurosci. 132 (2018) 388–395, https://doi.org/10.1037/bne0000223.

[9] C.S. Keene, D.J. Bucci, Contributions of the retrosplenial and posterior parietal cortices to cue-specific and contextual fear conditioning, Behav. Neurosci. 135 (2021) 693–701, https://doi.org/10.1037/bne0000435.

[10] E.L. Sigwald, M.E. Genoud, M. Giachero, S. de Olmos, V.A. Molina, A. Lorenzo, Selective neuronal degeneration in the retrosplenial cortex impairs the recall of contextual fear memory, Brain Struct. Funct. 221 (2016) 1861–1875, https://doi.org/10.1007/S00429-015-1008-9.

[11] K.K. Cowansage, T. Shuman, B.C. Dillingham, A. Chang, P. Golshani, M. Mayford, Direct reactivation of a coherent neocortical memory of context, Neuron 84 (2014) 432–441, https://doi.org/10.1016/J.NEURON.2014.09.022.

[12] T.P. Todd, M.L. Mehlman, C.S. Keene, N.E. De Angeli, D.J. Bucci, Retrosplenial cortex is required for the retrieval of remote memory for auditory cues, Learn. Mem. 23 (2016) 278–288, https://doi.org/10.1101/LM.041822.116.

[13] J.L. Kwapis, T.J. Jarome, J.L. Lee, M.R. Gilmartin, F.J. Helmstetter, Extinguishing trace fear engages the retrosplenial cortex rather than the amygdala, Neurobiol. Learn. Mem. 113 (2014) 41–54, https://doi.org/10.1016/J.NLM.2013.09.007.

[14] P.C. Holland, M.E. Bouton, Hippocampus and context in classical conditioning, Curr. Opin. Neurobiol. 9 (1999) 195–202, https://doi.org/10.1016/S0959-4388(99)80027-0.

[15] A. Talk, E. Stoll, M. Gabriel, Cingulate cortical coding of context-dependent latent inhibition, Behav. Neurosci. 119 (2005) 1524–1532, https://doi.org/10.1037/0735-7044.119.6.1524.

[16] K.A. Corcoran, B.J. Frick, J. Radulovic, L.M. Kay, Analysis of coherent activity between retrosplenial cortex, hippocampus, thalamus, and anterior cingulate cortex during retrieval of recent and remote context fear memory, Neurobiol. Learn. Mem. 127 (2016) 93–101, https://doi.org/10.1016/J.NLM.2015.11.019.

[17] M. Goto, L.W.W. Swanson, N.S.S. Canteras, Connections of the nucleus incertus, J Comp Neurol 438 (2001) 86–122, https://doi.org/10.1002/cne.1303.

[18] F.E. Olucha-Bordonau, V. Teruel, J. Barcia-González, A. Ruiz-Torner, A. A. Valverde-Navarro, F. Martínez-Soriano, Cytoarchitecture and efferent projections of the nucleus incertus of the rat, J Comp Neurol 464 (2003) 62–97, https://doi.org/10.1002/cne.10774.

[19] T.C.D. Burazin, R.A.D. Bathgate, M. Macris, S. Layfield, A.L. Gundlach, G. W. Tregear, Restricted, but abundant, expression of the novel rat gene-3 (R3) relaxin in the dorsal tegmental region of brain, J. Neurochem. 82 (2002) 1553–1557, https://doi.org/10.1046/j.1471-4159.2002.01114.x.

[20] M. Tanaka, N. Iijima, Y. Miyamoto, S. Fukusumi, Y. Itoh, H. Ozawa, Y. Ibata, Neurons expressing relaxin 3/INSL 7 in the nucleus incertus respond to stress, Eur. J. Neurosci. 21 (2005) 1659–1670, https://doi.org/10.1111/j.1460-9568.2005.03980.x.

[21] S. Ma, P. Bonaventure, T. Ferraro, P.-J.-J. Shen, T.C.D. Burazin, R.A.D. Bathgate, C. Liu, G.W. Tregear, S.W. Sutton, A.L. Gundlach, Relaxin-3 in GABA projection neurons of nucleus incertus suggests widespread influence on forebrain circuits via G-protein-coupled receptor-135 in the rat, Neuroscience 144 (2007) 165–190, https://doi.org/10.1016/j.neuroscience.2006.08.072.

[22] N. Nasirova, L.A. Quina, G. Morton, A. Walker, E.E. Turner, Mapping cell types and efferent pathways in the ascending relaxin-3 system of the nucleus incertus, eNeuro (2020), https://doi.org/10.1523/eneuro.0272-20.2020.

[23] I. Gil-Miravet, Á. Núñez-Molina, M. Navarro-Sánchez, E. Castillo-Gómez, F. Ros-Bernal, A.L. Gundlach, F.E. Olucha-Bordonau, Nucleus incertus projections to rat medial septum and entorhinal cortex: rare collateralization and septal-gating of temporal lobe theta rhythm activity, Brain Struct. Funct. 228 (2023) 1307–1328, https://doi.org/10.1007/s00429-023-02650-x.

[24] S. Ma, F.E. Olucha-Bordonau, A. Hossain, F. Lin, C. Kuei, C. Liu, J.D. Wade, S. W. Sutton, A. Nuñez, A.L. Gundlach, M.A. Hossain, F. Lin, C. Kuei, C. Liu, J. D. Wade, S.W. Sutton, A. Nunez, A.L. Gundlach, A. Nuñez, A.L. Gundlach, Modulation of hippocampal theta oscillations and spatial memory by relaxin-3 neurons of the nucleus incertus, Learn. Mem. 16 (2009) 730–742, https://doi.org/10.1101/lm.1438109.

[25] A. Nuñez, A. Cervera-Ferri, F.E. Olucha-Bordonau, A. Ruiz-Torner, V. Teruel, Nucleus incertus contribution to hippocampal theta rhythm generation, Eur. J. Neurosci. 23 (2006) 2731–2738, https://doi.org/10.1111/j.1460-9568.2006.04797.x.

[26] C.W. Pereira, F.N. Santos, A. Sánchez-Pérez, M. Otero-García, M. Marchioro, S. Ma, A.L. Gundlach, F.E. Olucha-Bordonau, Electrolytic lesion of the nucleus incertus retards extinction of auditory conditioned fear, Behav. Brain Res. 247 (2013) 201–210, https://doi.org/10.1016/j.bbr.2013.03.025.

[27] A. Szőnyi, K.E. Sos, R. Nyilas, D. Schlingloff, A. Domonkos, V.T. Takács, B. Pósfai, P. Hegedüs, J.B. Priestley, A.L. Gundlach, A.I. Gulyás, V. Varga, A. Losonczy, T.F. Freund, G. Nyiri, Brainstem nucleus incertus controls contextual memory formation, Science (1979) 364 (2019) eaaw0445. https://doi.org/10.1126/science.aaw0445.

[28] T.N. Wilkinson, R.A.D. Bathgate, The evolution of the relaxin peptide family and their receptors, Adv. Exp. Med. Biol. 612 (2007) 1–13, https://doi.org/10.1007/978-0-387-74672-2_1.

[29] C. Liu, E. Eriste, S. Sutton, J. Chen, B. Roland, C. Kuei, N. Farmer, H. Jörnvall, R. Sillard, T.W. Lovenberg, Identification of relaxin-3/INSL7 as an endogenous ligand for the orphan G-protein-coupled receptor GPCR135, J. Biol. Chem. 278 (2003) 50754–50764, https://doi.org/10.1074/jbc.M308995200.

[30] R.A.D. Bathgate, R. Ivell, B.M. Sanborn, O.D. Sherwood, R.J. Summers, International Union of Pharmacology LVII: recommendations for the nomenclature of receptors for relaxin family peptides, Pharmacol. Rev. 58 (2006) 7–31, https://doi.org/10.1124/pr.58.1.9.

[31] E.T. Van der Westhuizen, T.D. Werry, P.M. Sexton, R.J. Summers, The relaxin family peptide receptor 3 activates extracellular signal-regulated kinase 1/2 through a protein kinase C-dependent mechanism, Mol. Pharmacol. 71 (2007) 1618–1629, https://doi.org/10.1124/mol.106.032763.

[32] H. Albert-Gascó, Á. García-Avilés, S. Moustafa, S. Sánchez-Sarasua, A.L. Gundlach, F.E. Olucha-Bordonau, A.M. Sánchez-Pérez, Central relaxin-3 receptor (RXFP3) activation increases ERK phosphorylation in septal cholinergic neurons and impairs spatial working memory, Brain Struct. Funct. 222 (2017) 449–463, https://doi.org/10.1007/s00429-016-1227-8.

[33] M. Haidar, G. Guèvremont, C. Zhang, R.A.D. Bathgate, E. Timofeeva, C.M. Smith, A.L. Gundlach, Relaxin-3 inputs target hippocampal interneurons and deletion of hilar relaxin-3 receptors in "floxed-RXFP3" mice impairs spatial memory, Hippocampus 27 (2017) 529–546, https://doi.org/10.1002/hipo.22709.

[34] M. Haidar, K. Tin, C. Zhang, M. Nategh, J. Covita, A.D.D. Wykes, J. Rogers, A. L. Gundlach, Septal GABA and glutamate neurons express RXFP3 mRNA and depletion of septal RXFP3 impaired spatial search strategy and long-term reference memory in adult mice, Front. Neuroanat. 13 (2019) 30, https://doi.org/10.3389/fnana.2019.00030.

[35] D.E. Ganella, P.J. Ryan, R.A.D. Bathgate, A.L. Gundlach, Increased feeding and body weight gain in rats after acute and chronic activation of RXFP3 by relaxin-3 and receptor-selective peptides, Behav. Pharmacol. 23 (2012) 516–525, https://doi.org/10.1097/FBP.0b013e3283576999.

[36] V. Rytova, D.E. Ganella, D. Hawkes, R.A.D. Bathgate, S. Ma, A.L. Gundlach, Chronic activation of the relaxin-3 receptor on GABA neurons in rat ventral hippocampus promotes anxiety and social avoidance, Hippocampus 29 (2019) 905–920, https://doi.org/10.1002/hipo.23089.

[37] F. Shabanpoor, M. Akhter Hossain, P.J. Ryan, A. Belgi, S. Layfield, M. Kocan, S. Zhang, C.S. Samuel, A.L. Gundlach, R.A.D. Bathgate, F. Separovic, J.D. Wade, Minimization of human relaxin-3 leading to high-affinity analogues with increased selectivity for relaxin-family peptide 3 receptor (RXFP3) over RXFP1, J. Med. Chem. 55 (2012) 1671–1681, https://doi.org/10.1021/jm201505p.

[38] J.D. Wade, F. Lin, M.A. Hossain, R.M. Dawson, Chemical synthesis and biological evaluation of an antimicrobial peptide gonococcal growth inhibitor, Amino Acids 43 (2012), https://doi.org/10.1007/s00726-012-1305-z.

[39] W. Li, N.M. O'Brien-Simpson, M.A. Hossain, J.D. Wade, The 9-Fluorenylmethoxycarbonyl (Fmoc) group in chemical peptide synthesis-its past, present, and future, Aust. J. Chem. 73 (2020), https://doi.org/10.1071/CH19427.

[40] C.S. Samuel, F. Lin, M.A. Hossain, C. Zhao, T. Ferraro, R.A.D. Bathgate, G. W. Tregear, J.D. Wade, Improved chemical synthesis and demonstration of the relaxin receptor binding affinity and biological activity of mouse relaxin, Biochemistry 46 (2007), https://doi.org/10.1021/bi700238h.

[41] S. Zhang, F. Lin, M.A. Hossain, F. Shabanpoor, G.W. Tregear, J.D. Wade, Simultaneous post-cysteine(S-Acm) group removal quenching of iodine and isolation of peptide by one step ether precipitation, Int. J. Pept. Res. Ther. (2008), https://doi.org/10.1007/s10989-008-9148-x.

[42] H. Albert-Gasco, S. Sanchez-Sarasua, S. Ma, C. García-Díaz, A.L. Gundlach, A. M. Sanchez-Perez, F.E. Olucha-Bordonau, Central relaxin-3 receptor (RXFP3) activation impairs social recognition and modulates ERK-phosphorylation in specific GABAergic amygdala neurons, Brain Struct. Funct. 224 (2019) 453–469, https://doi.org/10.1007/s00429-018-1763-5.

[44] J. Sugar, M.P. Witter, N.M. van Strien, N.L.M. Cappaert, The retrosplenial cortex: intrinsic connectivity and connections with the (para)hippocampal region in the rat. An interactive connectome, Front Neuroinform 5 (2011) 7, https://doi.org/10.3389/fninf.2011.00007.

[45] H. Albert-Gascó, S. Ma, F. Ros-Bernal, A.M. Sánchez-Pérez, A.L. Gundlach, F. E. Olucha-Bordonau, GABAergic neurons in the rat medial septal complex express relaxin-3 receptor (RXFP3) mRNA, Front. Neuroanat. 11 (2018) 133, https://doi.org/10.3389/fnana.2017.00133.
[46] F.E. Olucha-Bordonau, M. Otero-Garcia, A.M. Sanchez-Perez, A. Nunez, S. Ma, A. L. Gundlach, Distribution and targets of the relaxin-3 innervation of the septal area in the rat, J. Comp. Neurol. 520 (2012) 1903–1939, https://doi.org/10.1002/cne.23018.
[47] F.N. Santos, C.W. Pereira, A.M. Sánchez-Pérez, M. Otero-García, S.K. Ma, A. L. Gundlach, F.E. Olucha-Bordonau, Comparative distribution of relaxin-3 inputs and calcium-binding protein-positive neurons in rat amygdala, Front. Neuroanat. 10 (2016) 36, https://doi.org/10.3389/fnana.2016.00036.
[48] T.P. Todd, D.I. Fournier, D.J. Bucci, Retrosplenial cortex and its role in cue-specific learning and memory, Neurosci. Biobehav. Rev. 107 (2019) 713–728, https://doi.org/10.1016/J.NEUBIOREV.2019.04.016.
[49] G.J. Quirk, G.K. Russo, J.L. Barron, K. Lebron, The role of ventromedial prefrontal cortex in the recovery of extinguished fear, J. Neurosci. 20 (2000) 6225–6231.
[50] D. Sierra-Mercado, N. Padilla-Coreano, G.J. Quirk, Dissociable roles of prelimbic and infralimbic cortices, ventral hippocampus, and basolateral amygdala in the expression and extinction of conditioned fear, Neuropsychopharmacology 36 (2011) 529–538, https://doi.org/10.1038/npp.2010.184.
[51] S. Robinson, C.E. Poorman, T.J. Marder, D.J. Bucci, Identification of functional circuitry between retrosplenial and postrhinal cortices during fear conditioning, J. Neurosci. 32 (2012) 12076–12086, https://doi.org/10.1523/JNEUROSCI.2814-12.2012.
[52] A. Kania, A. Gugula, A. Grabowiecka, C. de Ávila, T. Blasiak, Z. Rajfur, M. H. Lewandowski, G. Hess, E. Timofeeva, A.L. Gundlach, A. Blasiak, Inhibition of oxytocin and vasopressin neuron activity in rat hypothalamic paraventricular nucleus by relaxin-3-RXFP3 signalling, J. Physiol. 595 (2017) 3425–3447, https://doi.org/10.1113/JP273787.
[53] A. Kania, A. Szlaga, P. Sambak, A. Gugula, E. Blasiak, M.V.M. Di Bonaventura, M. A. Hossain, C. Cifani, G. Hess, A.L. Gundlach, A. Blasiak, RLN3/RXFP3 signaling in the PVN inhibits magnocellular neurons via M-like current activation and contributes to binge eating behavior, J. Neurosci. 40 (2020) 5362–5375, https://doi.org/10.1523/JNEUROSCI.2895-19.2020.
[54] D.L. Greene, N. Hoshi, Modulation of Kv7 channels and excitability in the brain, Cell Mol Life Sci 74 (2017) 495–508, https://doi.org/10.1007/s00018-016-2359-y.
[55] M. Cammarota, L.R.M. Bevilaqua, P. Ardenghi, G. Paratcha, M. Levi de Stein, I. Izquierdo, J.H. Medina, Learning-associated activation of nuclear MAPK, CREB and Elk-1, along with Fos production, in the rat hippocampus after a one-trial avoidance learning: abolition by NMDA receptor blockade, Mol. Brain Res. 76 (2000) 36–46, https://doi.org/10.1016/S0169-328X(99)00329-0.
[56] U. Frey, Y.Y. Huang, E.R. Kandel, Effects of cAMP simulate a late stage of LTP in hippocampal CA1 neurons, Science 260 (1993) (1979) 1661–1664, https://doi.org/10.1126/science.8389057.
[57] S. Impey, D.M. Smith, K. Obrietan, R. Donahue, C. Wade, D.R. Storm, Stimulation of cAMP response element (CRE)-mediated transcription during contextual learning, Nat. Neurosci. 1 (1998) 595–601, https://doi.org/10.1038/2830.
[58] S. Ha, I.-J. Sohn, N. Kim, H.J. Sim, K.-A. Cheon, Characteristics of brains in autism spectrum disorder: structure, function and connectivity across the lifespan, Exp Neurobiol 24 (2015) 273–284, https://doi.org/10.5607/en.2015.24.4.273.
[59] K.A. Corcoran, K. Leaderbrand, J. Radulovic, Extinction of remotely acquired fear depends on an inhibitory NR2B/PKA pathway in the retrosplenial cortex, J. Neurosci. 33 (2013) 19492–19498, https://doi.org/10.1523/JNEUROSCI.3338-13.2013.
[60] K. Leaderbrand, K.A. Corcoran, J. Radulovic, Co-activation of NR2A and NR2B subunits induces resistance to fear extinction, Neurobiol. Learn. Mem. 113 (2014) 35–40, https://doi.org/10.1016/J.NLM.2013.09.005.
[61] I. Gil-Miravet, A. Mañas-Ojeda, F. Ros-Bernal, E. Castillo-Gómez, H. Albert-Gascó, A.L. Gundlach, F.E. Olucha-Bordonau, Involvement of the nucleus incertus and relaxin-3/RXFP3 signaling system in explicit and implicit memory, Front. Neuroanat. 15 (2021) 637922. http://www.ncbi.nlm.nih.gov/pubmed/33867946.
[62] J. Ji, S. Maren, Hippocampal involvement in contextual modulation of fear extinction, Hippocampus 17 (2007) 749–758, https://doi.org/10.1002/hipo.20331.
[63] J.H. Lee, W. Bin Kim, E.H. Park, J.H. Cho, Neocortical synaptic engrams for remote contextual memories, Nat. Neurosci. 26 (2023), https://doi.org/10.1038/s41593-022-01223-1.
[64] P.J. Ryan, S. Ma, F.E. Olucha-Bordonau, A.L. Gundlach, Nucleus incertus - An emerging modulatory role in arousal, stress and memory, Neurosci. Biobehav. Rev. 35 (2011) 1326–1341, https://doi.org/10.1016/j.neubiorev.2011.02.004.